

Functional Optimal Transport: Mapping Estimation and Domain Adaptation for Functional data

Jiacheng Zhu ^{*1} Aritra Guha ^{*2} Mengdi Xu ¹ Yingchen Ma ³ Rayleigh Lei ⁴ Vincenzo Loffredo ⁴
XuanLong Nguyen ⁴ Ding Zhao ¹

Abstract

Optimal transport (OT) has generated much recent interest by its capability of finding mappings that transport mass from one distribution to another, and found useful roles in machine learning tasks such as unsupervised learning, domain adaptation and transfer learning. On the other hand, in many applications data are generated by complex mechanisms involving convoluted spaces of functions, curves and surfaces in high dimensions. Functional data analysis provides a useful framework of treatment for such domains. In this paper we introduce a novel formulation of optimal transport problem in functional spaces and develop an efficient learning algorithm for finding the stochastic map between functional domains. We apply our method to synthetic datasets and study the geometric properties of the transport map. Experiments on real-world datasets of robot arm trajectories and digit numbers further demonstrate the effectiveness of our method on applications of domain adaptation and generative modeling.

1. Introduction

Optimal transport is a powerful formalism for finding and quantifying the movement of mass from one probability distribution to another (Villani, 2008). In recent years, it has been instrumental in a variety of important machine learning tasks, including deep generative modeling (Arjovsky et al., 2017; Salimans et al., 2018), unsupervised learning (Ho et al., 2017; Mallasto & Feragen, 2017) and domain adaptations (Ganin & Lempitsky, 2015; Bhushan Damodaran et al., 2018). As machine learning algorithms are applied

to increasingly complex data domains, it is of great interest to develop optimal transport based methods and tools for complex data structures. A particularly common form of such data structures is functional data — data that may be viewed as random samples of (relatively) smooth functions, curves or surfaces in high dimension spaces (Mirshani et al., 2019; Hsing & Eubank, 2015). Examples of real-world machine learning applications involving functional data are numerous, ranging from robotics (Deisenroth et al., 2013) and natural language processing (Rodrigues et al., 2014) to economics (Horváth & Kokoszka, 2012) and healthcare (Chan et al., 2020).

The goal of this paper is to provide a novel formulation of the optimal transport problem in function spaces¹, to develop an efficient learning algorithm for finding a suitable notion of optimal stochastic map that transports samples from one functional domain to another, and to demonstrate the effectiveness of our approach to several application domains where the functional optimal transport viewpoint proves natural and useful. There are several technical challenges arising in our problem: both the source and the target function spaces can be very complex, and in general of infinite dimensions. Moreover, one needs to deal with the distributions over such spaces, which is difficult if one is to model them. In general, the optimal coupling or the underlying optimal transport map between the two distributions is hard to characterize and compute efficiently. Yet, to be useful one must find an explicit transport map that can approximate reasonably well the optimal coupling (the original Monge problem) (Villani, 2008; Perrot et al., 2016).

There is indeed a growing interest in finding an explicit optimal transport map linked to the Monge problem. A large amount of work was conducted to scale up the computation of the transport map (Genevay et al., 2016; Meng et al., 2019), including approximating transport maps with neural networks (Seguy et al., 2017; Makuva et al., 2019), deep generative models (Xie et al., 2019) and flow models (Huang et al., 2020). The most existing approaches learn a mapping that transports point mass from one (empirical) distribution to another. There is scarcely any work that ad-

^{*}Equal contribution ¹Department of Mechanical Engineering, Carnegie Mellon University ²Department of Statistical Science, Duke University ³College of Literature, Science, and the Arts, University of Michigan ⁴Department of Statistics, University of Michigan. Correspondence to: Jiacheng Zhu <jzhu4@andrew.cmu.edu>, Aritra Guha <aritra.guha@duke.edu>.

¹Code is available here: <https://github.com/VersElectronics/FOT>

dresses optimal transport in the domains of functions by specifically accounting for the functional data structure.

The mathematical machinery of functional data analysis (FDA) (Hsing & Eubank, 2015), along with recent advances in computational optimal transport via regularization techniques (e.g., (Cuturi, 2013)) will be brought to bear on the aforementioned problems. First, we take a model-free approach, by avoiding making assumptions on the source and target distributions of functional data. Instead, we aim for learning the (stochastic) transport map directly. Second, if we follow the FDA’s perspective, both the source and target distributions are supported on suitable Hilbert spaces of functions. A transport map between two Hilbert spaces H_1 and H_2 will be represented by a class of linear operators, namely the integral operators. In fact, we shall restrict ourselves to Hilbert-Schmidt operators, which are compact and computationally convenient to regularize. Finally, the optimal (deterministic) transport map between two probability measures on function spaces may not exist. Thus, we enlarge the space of transport maps by allowing for stochastic coupling between the two domains H_1 and H_2 , while controlling the complexity of such coupling via the entropic regularization technique initiated by (Cuturi, 2013).

It is interesting to note that our formulation admits two complementary interpretations: it can be viewed as learning an integral operator regularized by a transport plan (a coupling distribution) or it can also be seen as an optimal coupling problem (the Kantorovich problem), which is associated with a cost matrix parametrized by the integral operator. In any case, we propose a joint optimization problem that estimates both the transport map and the coupling distribution. This problem is block coordinate-wise convex, and admits an efficient algorithm for finding explicit transport map that can be applied on sampled functions. We first demonstrate empirical evidence for the effectiveness of our approach on synthetic datasets for smooth function data. Then, we provide a suite of experiments on domain adaptation and generative modeling with real-world data.

The paper proceeds as follows. Section 2 reviews preliminary backgrounds of optimal transport and functional data analysis. Section 3 discusses the notion transportation maps as elements of a Hilbert space, setting stage for our functional OT framework and optimization algorithm for finding the transportation map on function spaces in Section 4. Section 5 discusses extensive experiments with synthetic and real data.

Notation: Given a probability measure μ and a Borel map T acting on the support of μ , $T_{\#}\mu$ denotes the push-forward operator of μ by T . For a probability vector (P_1, \dots, P_i, \dots) , its *negative* entropy function is defined as $H(\mathbf{P}) := \sum_i P_i \log P_i$. An inner product relative to a Hilbert space H is denoted by $\langle \cdot, \cdot \rangle_H$. For a set X

endowed with a probability measure ρ , $L^2(X, \rho)$ is defined as the space of square integrable functions with norm $\|f\|_{\rho}^2 = \langle f, f \rangle_{\rho} = \int_X |f(x)|^2 d\rho(x)$. $\|\cdot\|_{HS}$ is the Hilbert-Schmidt operator norm defined in Section 2. The outer product operator between two elements $e_i \in H_i$ for $i = 1, 2$ is denoted by $e_1 \otimes_1 e_2 : H_1 \rightarrow H_2$ and is defined by $(e_1 \otimes_1 e_2)f = \langle e_1, f \rangle_{H_1} e_2$ for $f \in H_1$.

2. Preliminaries

In this section, we briefly review some background knowledge on optimal transport and functional data analysis.

2.1. Optimal transport

Monge problem Let $\mathcal{X} \subseteq \mathbb{R}^{d_s}$ and $\mathcal{Y} \subseteq \mathbb{R}^{d_t}$ be two complete and separable metric spaces and $\mathcal{M}(\mathcal{Z})$ denote the space of probability measures over spaces \mathcal{Z} . Given two probability measures $\mu \in \mathcal{M}(\mathcal{X})$, $\nu \in \mathcal{M}(\mathcal{Y})$ and a cost function $c : \mathcal{X} \times \mathcal{Y} \mapsto \mathbb{R}^+$, the Monge problem consists in finding a Borel map, $T : \mathcal{X} \mapsto \mathcal{Y}$ between μ and ν that realizes the infimum

$$\inf_T \int_{\Omega} c(x, T(x)) d\mu(x) \quad \text{subject to } T_{\#}\mu = \nu, \quad (1)$$

where $T_{\#}\mu$ denotes the push forward operator of μ by T . The existence of the optimal transport map T is not always guaranteed: the Monge problem is non-convex and often unfeasible, for example, when the support μ and ν are different number of Diracs. Monge’s formulation can be improved by the following relaxation problem by Kantorovich (Kantorovich, 1958).

Kantorovich relaxation Given $\mu \in \mathcal{M}(\mathcal{X})$, $\nu \in \mathcal{M}(\mathcal{Y})$ and a cost function $c : \mathcal{X} \times \mathcal{Y} \mapsto \mathbb{R}^+$, Kantorovich OT seeks a joint measure $\pi \in \Pi$ minimizing

$$W(\mu, \nu) := \inf_{\pi \in \Pi} \int_{\mathcal{X} \times \mathcal{Y}} c(x, y) d\pi(x, y). \quad (2)$$

Here, Π is the set of couplings of μ and ν denoted by :

$$\Pi = \{\pi : \gamma_{\#}^{\mathcal{X}} \pi = \mu, \gamma_{\#}^{\mathcal{Y}} \pi = \nu\}, \quad (3)$$

where $\gamma^{\mathcal{X}}, \gamma^{\mathcal{Y}}$ are functions that project onto \mathcal{X} and \mathcal{Y} respectively. Note that the optimal coupling always exists, and the conditional probability distributions $\pi_{y|x}$ gives stochastic maps from \mathcal{X} to \mathcal{Y} and is considered as “one-to-many” version of the deterministic map of the Monge map.

The computation in high dimensions of the optimal transport is typically computationally intensive. A faster approximate solution was proposed by (Cuturi, 2013) as follows:

$$\inf_{\pi \in \Pi} \int_{\mathcal{X} \times \mathcal{Y}} c(x, y) d\pi(x, y) + \lambda H(\pi). \quad (4)$$

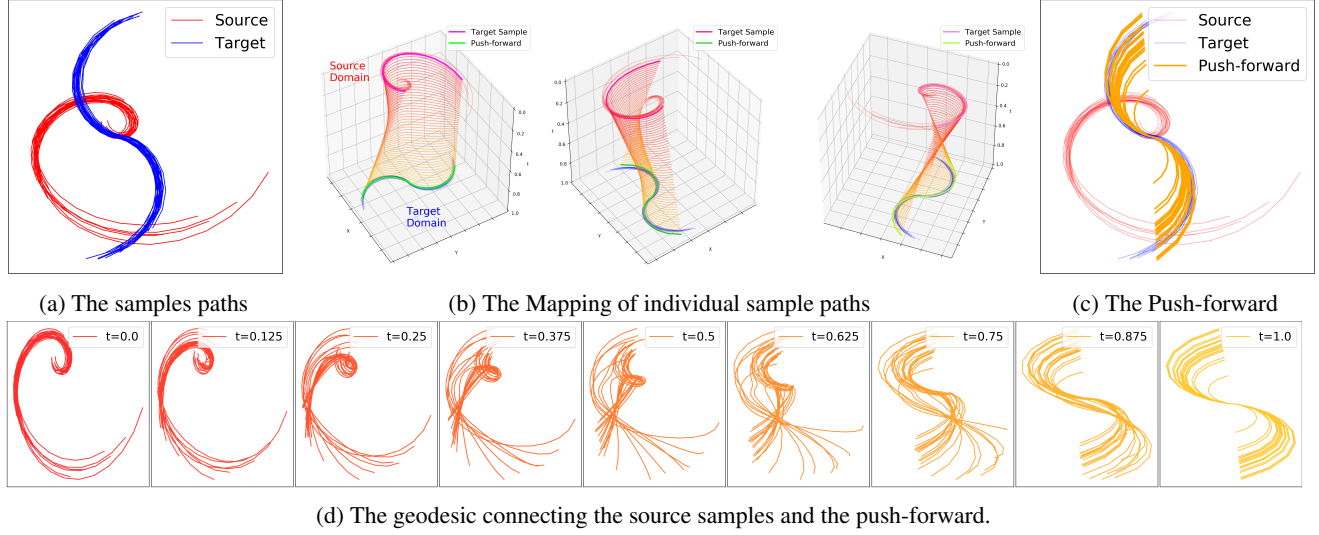


Figure 1: Illustration of the estimated map that pushes forward sample paths from the source **Swiss-roll curve dataset** to the target **Blue curve dataset**. (a) Datasets are a collection of continuous sample paths. (b) Three individual samples are mapped from source to target. (c) The resulting push-forward of all samples. (d) The geodesic implies a smooth mapping.

Here, $H(\pi) = \int \pi(x, y) \log(\pi(x, y)) dx dy$ is the negative entropy function of π .

While the Monge map is non-convex, the Kantorovich map can be non-deterministic especially when one of the marginal measures μ, ν is discrete. In this paper we consider the following problem: Find a Borel map $T : \mathcal{X} \mapsto \mathcal{Y}$ and a coupling $\pi \in \Pi$ that attains the infimum

$$\inf_{\pi \in \Pi, T} \int_{\mathcal{X} \times \mathcal{Y}} c(T(x), y) d\pi(x, y). \quad (5)$$

The following lemma establishes a connection between the Monge map in Eq. (1) and the optimal map in Eq. (5).

Lemma 1 *Let $c(\cdot, \cdot)$ be a norm on \mathcal{Y} . If there exists a Monge map, T , that attains the infimum in Eq. (1), and π that attains the infimum in Eq. (2), then T satisfies,*

$$\inf_{\pi \in \Pi} \int_{\mathcal{X} \times \mathcal{Y}} c(T(x), y) d\pi(x, y) = 0. \quad (6)$$

Thus, if $T', \pi' = \arg \inf_{\pi \in \Pi, T} \int_{\mathcal{X} \times \mathcal{Y}} c(T(x), y) d\pi(x, y)$, then $T = T'$ μ -a.s. and $\pi = \pi'$.

2.2. Functional data analysis

Functional data analysis adopts the perspective that certain types of data can be viewed as samples of random functions, which are given as random elements taking value in Hilbert spaces. Thus, data analysis techniques on functional data involve operations acting on Hilbert spaces of functions.

Linear operators on Hilbert spaces We recall some useful notions for operators from functional analysis. Let

$A : H_1 \mapsto H_2$ be a (linear) bounded operator, where H_1 (respectively, H_2) is a Hilbert space equipped with scalar product $\langle \cdot, \cdot \rangle_{H_1}$ (respectively, $\langle \cdot, \cdot \rangle_{H_2}$) and $(e_{1i})_{i \geq 1}$ ($(e_{2i})_{i \geq 1}$) is the Hilbert basis in H_1 (H_2). A is said to be Hilbert-Schmidt if $\sum_{i \geq 1} \|Ae_{1i}\|_{H_2}^2 < \infty$ for any Hilbert basis $(e_{1i})_{i \geq 1}$. The space of Hilbert-Schmidt operators between H_1 and H_2 , denoted $\mathcal{B}_{HS}(H_1, H_2)$ is also a Hilbert space endowed with the scalar product $\langle A, B \rangle_{HS} = \sum_i \langle Ae_{1i}, Be_{1i} \rangle_{H_2}$ and the corresponding Hilbert-Schmidt norm is denoted by $\|\cdot\|_{HS}$.

An important fact of Hilbert-Schmidt operators is given as follows (cf. Theorem 4.4.5 of (Hsing & Eubank, 2015)).

Theorem 1 *The linear space $\mathcal{B}_{HS}(H_1, H_2)$ is a separable Hilbert space when equipped with the HS inner product. For any choice of Complete Orthonormal Basis system (CONS) $\{e_{1i}\}$ and $\{e_{2j}\}$ for H_1 and H_2 respectively, $\{e_{1i} \otimes e_{2j}\}$ forms a CONS for $\mathcal{B}_{HS}(H_1, H_2)$.*

The following is an useful consequence of Theorem 1.

Corollary 1 *Any Hilbert-Schmidt operator $\Gamma : H_1 \mapsto H_2$ can be written as*

$$\Gamma = \sum_{i,j=1}^{\infty} \lambda_{i,j} e_{1i} \otimes e_{2j}, \quad (7)$$

where $\lambda_{i,j}$ are the coefficients associated with the $e_{1i} \otimes e_{2j}$ operators.

3. Optimal transport on Hilbert spaces

We proceed to provide a formulation of optimal transport in spaces of function, reposing on the foundation of functional

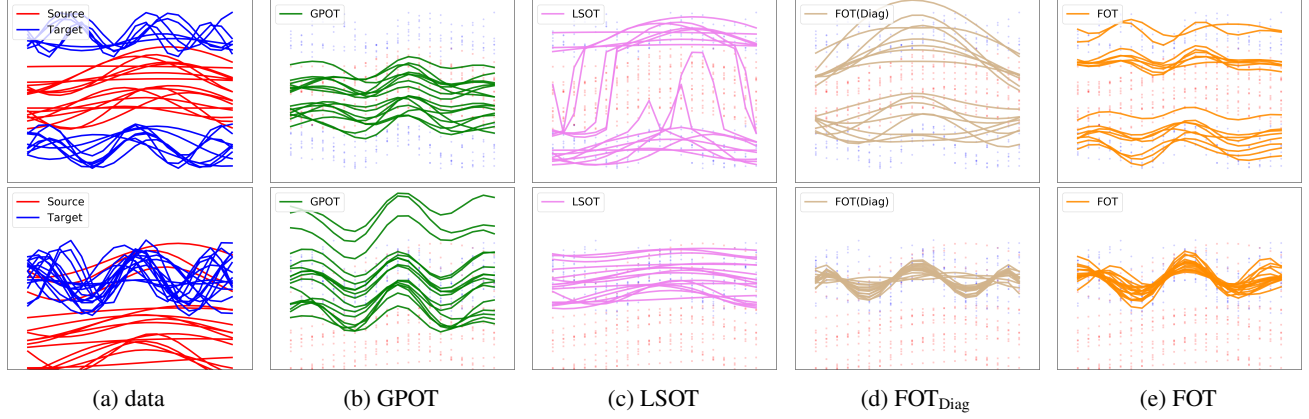


Figure 2: Push forward results learned by various approaches on mixture of sine dataset. (a) Sample functions from **source** and **target** domain. The resulting push-forwards of GPOT (b) and LSOT (c). FOT with diagonal Λ restriction; (e)FOT.

data analysis (FDA). In many application domains, data can be naturally viewed as samples from random functions embedded in high-dimensional ambient spaces. As a concrete example, in the domain of (vehicle) transportation, the trajectory of an object’s motion can be generally modeled as curves denoted by $f : \mathbb{R}^+ \rightarrow \mathbb{R}^d$ for some $d \geq 2$. $f(t)$ represents the location of the object at time t . For a vehicle, $d = 2$; for a robot’s arm motion $d = 3$, and so on.

3.1. Trajectories as Hilbert space elements

Suppose one is interested in the relations and transformations of motion patterns across different environments (ambient spaces). More specifically, given motion pattern in environments E_1 and E_2 , one may wish to find a map Γ that outputs a motion pattern in environment E_2 when the input is a motion pattern in E_1 . The map provides a method to produce samples in E_2 given access to a collection of motion patterns in E_1 and a few samples in E_2 . Moreover, Γ also encodes structural differences in the environments. A natural way to do this is to model each motion pattern as an element embedded in an Hilbert space of functions.

Formally, given Hilbert spaces of function H_1 and H_2 , and let $\mathcal{F}_1 \subseteq H_1$, $\mathcal{F}_2 \subseteq H_2$. In addition, \mathcal{F}_1 and \mathcal{F}_2 are endowed with Borel probability measures μ and ν , respectively. We wish to find a Borel map $\Gamma : \mathcal{F}_1 \mapsto \mathcal{F}_2$ such that, if $f \sim \mu$ represents a random motion pattern in \mathcal{F}_1 , then Γf is the correspond random motion pattern in \mathcal{F}_2 that satisfies $\Gamma f \sim \nu$. As noted in Section 2, such a map may not always exist, but this motivates the following formulation.

3.2. Optimization problem

For mathematical and computational tractability, we restrict the map Γ to the space of Hilbert-Schmidt operators, and

define

$$\Gamma := \arg \inf_{T \in \mathcal{B}_{HS}(H_1, H_2)} W_2(T_{\#}\mu, \nu), \quad (8)$$

where $\Gamma_{\#}\mu$ is the push-forward of μ by Γ . The space of solutions of Eq. (8) may still be large; thus we consider imposing a shrinkage penalty via the following problem:

$$\Gamma = \arg \inf_{T \in \mathcal{B}_{HS}(H_1, H_2)} W_2^2(T_{\#}\mu, \nu) + \eta \|T\|_{HS}^2, \quad (9)$$

By Corollary 1, any Hilbert-Schmidt operator $T \in \mathcal{B}_{HS}(H_1, H_2)$ can be represented as $T = \sum_{i,j=1}^{\infty} \lambda_{i,j} e_{1i} \otimes e_{2j}$. Moreover, since the Hilbert-Schmidt operators are compact and bounded, there exists a *singular value decomposition* (Mollenhauer et al., 2020) given by

$$\Gamma = \sum_{i \in I} \sigma_i (v_i \otimes u_i) \quad (10)$$

where I is an either finite or countably infinite order index set, $\{u_i\}_{i \in I} \subset H_1$ and $\{v_i\}_{i \in I} \subset H_2$ two orthonormal systems, and $\{\sigma_i\}_{i \in I} \subset \mathbb{R}$ the set of singular values.

Lemma 2 provides an expression to explicitly calculate the Hilbert-Schmidt norm for a Hilbert-Schmidt operator.

Lemma 2 *Let $\{e_{1i}\}, \{e_{2i}\}$ be a Complete Orthonormal System for H_1, H_2 respectively. Then any Hilbert-Schmidt operator $T \in \mathcal{B}_{HS}(H_1, H_2)$ can be decomposed as:*

$$T = \sum_{i,j} \lambda_{i,j} e_{1i} \otimes e_{2j}. \quad (11)$$

Moreover, in this case,

$$\|T\|_{HS}^2 = \sum_{i,j} \lambda_{i,j}^2. \quad (12)$$

The optimal Γ obtained in Eq. (9) is intricately connected with the optimal coupling between μ and ν . In other words, if $T', \tilde{\pi}$ attains the infimum of :

$$\inf_{\pi \in \Pi, T} \int_{\mathcal{F}_1 \times \mathcal{F}_2} \|Tf_1 - f_2\|_{H_2}^2 d\pi(f_1, f_2) + \eta \|T\|_{HS}^2, \quad (13)$$

then $T' = \Gamma$ a.s. μ . In the next section we provide explicit computation for the optimization problem in Eq. (13) for finite dimensional spaces.

4. Methodology

The previous section describes infinite-dimensional generalization of compact operators on Hilbert spaces. However, in practice, we always deal with finite dimensional objects. Therefore, in this section we assume the following:

1. \mathcal{F}_1 and \mathcal{F}_2 are finite dimensional Hilbert spaces of dimensions d_1 and d_2 respectively.
2. The source and target dataset on \mathcal{F}_1 , resp. \mathcal{F}_2 , comprises of samples of N (resp. n with $n \ll N$) functions $f_{11}, \dots, f_{1N} \sim \mu$ ($f_{21}, \dots, f_{2n} \sim \nu$).

Problem: Our goal is to simultaneously learn the joint distribution (coupling) π and an integral operator Γ as the transport map via Eq. (13) adapted to the above setting. Additionally, we also impose certain penalties to satisfy other criteria as described below.

- (i) Eq. (13) involves solving an optimal coupling problem for each T , and therefore we choose to add an entropic penalty to our objective function to improve computational performance as identified in (Cuturi, 2013).
- (ii) Let the coupling matrix be denoted by $(\pi_{l,k})_{l,k}$. Additional to the entropic penalty, we also impose an l_p penalty on the coupling matrix via the term $-\gamma_p \sum_{l=1}^N \sum_{k=1}^n \pi_{l,k}^p$. The usefulness of this penalty is two-fold.
 - (a) It ensures that the optimal coupling $(\pi_{l,k})$ has fewer active parameters thereby easing computing for large datasets.
 - (b) Secondly, in combination with the entropic penalization, one can think of this as imposing a robustness in addition to shrinkage. Similar behavior is observed for the Huber loss (Huber, 1964).

Objective and Optimization: In consideration of condition (i) and (ii) above, the objective function to be optimized

Algorithm 1 Joint Learning of Λ and Π

Input: Observed functional data $\{\mathbf{f}_{1i}\}_{i=1}^{n_1}$ and $\{\mathbf{f}_{2j}\}_{j=1}^{n_2}$, coefficient γ_h, γ_p, η , and learning rate l_r .

Initial value $\Lambda_0 \leftarrow \Lambda_{ini}$, $\Pi_0 \leftarrow \Pi_{ini}$.

Obtain CONS: \mathbf{U} and \mathbf{V} with SVD (Eq. 10)

for $t = 1$ **to** T_{\max} **do**

 # Step 1. Update Λ_{t-1} with gradient descent

$g_\Lambda \leftarrow \nabla_\Lambda L(\Lambda, \Pi)$, $\Lambda_t \leftarrow \Lambda_{t-1} + l_r g_\Lambda$

 # Step 2. Update Π_{t-1}

if Use Sinkhorn **then**

$\mathbf{C}_{l,k} \leftarrow \|\mathbf{V}\Lambda_t\mathbf{U}^T\mathbf{f}_{1l} - \mathbf{f}_{2k}\|_2^2$ # Cost matrix

$\Pi_t \leftarrow \text{Sinkhorn}(\gamma_h, \mathbf{C} \in \mathbb{R}^{N \times n})$

else

$\Pi_t \leftarrow \text{argmin}_{\Pi} \mathcal{L}(\Pi, \Lambda; \rho)$

end if

end for

Output: $\Pi_{T_{\max}}$, $\Lambda_{T_{\max}}$

can be seen to be:

$$\begin{aligned} \min_{\mathbf{T}, \pi} & \sum_{l=1}^N \sum_{k=1}^n \pi_{l,k} C_{lk}(\mathbf{T}) + \eta \|\mathbf{T}\|_{HS}^2 \\ & + \gamma_h \sum_{l,k} \pi_{l,k} \log \pi_{l,k} - \gamma_p \sum_{l=1}^N \sum_{k=1}^n \pi_{l,k}^p \\ \text{s.t. } & \mathbf{T} \in \mathcal{B}_{HS}, \quad \pi \in \Pi(N, n), \end{aligned} \quad (14)$$

where $C_{lk}(\mathbf{T}) := d(\mathbf{T}\mathbf{f}_{1l}, \mathbf{f}_{2k})$, $\gamma_p, \gamma_h > 0$ and $p > 1$ and $d(\cdot, \cdot)$ is a distance metric in \mathbb{F}_2 . Also, $\Pi(N, n) := \{\pi \in (\mathbb{R}^+)^{N \times n} \mid \pi \mathbf{1}_n = \mathbf{1}_N/N, \pi^T \mathbf{1}_N = \mathbf{1}_n/n\}$ with $\mathbf{1}_n$ a length n vector of ones. The term $-\gamma_p \sum_{l,k} \pi_{l,k}^p$ regularizes π so that the coupling better specifies the connection between the source and target distribution.

For further simplification, notice that \mathcal{F}_1 and \mathcal{F}_2 are finite dimensional spaces with CONS $\{e_{1i}\}_1^{d_1}, \{e_{2j}\}_1^{d_2}$ respectively, and therefore are isomorphically isometric to \mathbb{R}^{d_1} and \mathbb{R}^{d_2} with CONS (say) $\{u_i\}_1^{d_1}, \{v_j\}_1^{d_2}$ respectively. Assume that we can represent the CONS as matrices \mathbf{U} and \mathbf{V} respectively with each column resembling an isometric isomorphism of a basis element. Moreover $f \in \mathcal{F}_1$ can be isometrically embedded in \mathbb{R}^{d_1} . We can therefore write

$$\begin{aligned} \mathbf{T}\mathbf{f} &= \sum_{i,j} \lambda_{ij} (e_{1i} \otimes e_{2j}) = \sum_{i,j} \lambda_{ij} \langle e_{1i}, \mathbf{f} \rangle_{\mathcal{F}_1} e_{2j} \\ &\cong \mathbf{V} \Lambda \mathbf{U}^T \mathbf{f} \end{aligned} \quad (15)$$

where $\Lambda = (\lambda_{ij})_{i,j}$. Moreover, following Eq.(12), $\|\mathbf{T}\|_{HS}^2 = \sum_{i,j} \lambda_{ij}^2$.

This simplifies the objective in Eq. (14) further as:

$$\begin{aligned} \min_{\Lambda, \pi} & \sum_{l=1}^N \sum_{k=1}^n \pi_{l,k} \|\mathbf{V} \Lambda \mathbf{U}^T \mathbf{f}_{1l} - \mathbf{f}_{2k}\|_2^2 + \eta \|\Lambda\|_F^2 \\ & + \gamma_h \sum_{i,j} \pi_{ij} \log \pi_{ij} - \gamma_p \sum_{l=1}^N \sum_{k=1}^n \pi_{l,k}^p \\ \text{s.t. } & \Lambda \in \mathbb{R}^{N \times n}, \pi \in \Pi(N, n) \end{aligned} \quad (16)$$

The above problem is convex in T and π separately. However, it is not convex jointly. To alleviate this problem of non-convexity we propose a coordinate-wise gradient descent approach to minimize the above function. The algorithm is described in Algorithm 1 and the explicit calculations are shown in the appendix. Experimental results for various settings with this algorithm are described in the following section.

5. Experiments

In this section, we evaluate our proposed Functional Optimal Transport on various tasks.

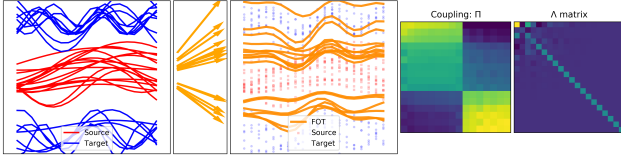


Figure 3: Illustration of the estimated map applied to a dataset, learned probabilistic coupling, and Λ matrix.

5.1. Pushing forward continuous sample functions

A driving motivation for the proposed Functional Optimal Transport (FOT) is to learn a map that pushes forward sample functions realized from a source to the target.

Dataset First, we qualitatively illustrate our approach on a synthetic dataset in which the source and target data samples are generated from a mixture of random functions. Each sample $\{y_i(x_i)\}_{i=1}^n$ is a realization evaluated from a random function $y_i = A_k \sin(\omega_k x_i + \phi_k) + m_k$ where the amplitude A_k , angular frequency ω_k , phase ϕ_k and translation m_k are random parameters generated from a probability distribution, i.e. $[A_k, \omega_k, \phi_k, m_k] \sim P(\theta_k)$, and θ_k is the prior parameter for each mixture component.

Push-forward From Figure 3, we can see that our method effectively learns a transport map that pushes forward sample functions from the source domain to the target. Figure 3 shows that the learned probabilistic coupling reveals the mixture structure because the coupling is the transport plan that guides the push-forward.

Baseline methods In Figure 2, we compare our method with the following baselines: (i) Transport map of Gaussian Processes (Mallasto & Feragen, 2017; Masarotto et al., 2019), (ii) Large-Scale Optimal Transport (LSOT) (Seguy et al., 2017). To find the transport map using GPOT, we first do a GP regression on both source and target set and then apply the closed-form transport map to each sample function in the source domain. Note that the LSOT method is not intended for functional data from stochastic processes so we treat the functional data as point cloud of high dimensional vectors when applying the LSOT method. We can see that our method successfully push forward source sample paths to match the target samples. However, GPOT only alters the oscillation of curves while LSOT ignores the continuity of curves. In Figure 2d we restrict the Λ matrix to be diagonal. Compared with figure 2e, we can see that the learned map is more expressive without this restriction.

Method	1 \rightarrow 1	1 \rightarrow 2	2 \rightarrow 1	2 \rightarrow 2	2 \rightarrow 3
GPOT	17.560	14.809	16.826	59.452	45.085
LSOT	133.434	122.995	117.832	849.408	763.682
FOT _{Diag}	3.599	17.624	4.249	63.531	41.209
FOT	2.873	14.517	2.995	57.777	35.759

Table 1: Quantitative comparison on mixture of continuous function dataset. In particular, Push-forward of FOT methods without the Diagonal restriction achieve the least Wasserstein distances.

5.2. Quantitative Comparison

We also present a quantitative comparison between our approach and the benchmarks. To enable a fair comparison, we use the following Wasserstein distance to indicate how well the push-forward of source samples match the target samples:

$$L = \min_{\Pi} \frac{1}{n_L} \sum_{l,k} d(\mathbf{T}(\mathbf{f}_{1l}), \mathbf{f}_{2k}) \Pi_{lk}. \quad (17)$$

Here, $d(\mathbf{x}, \mathbf{y}) := \|\mathbf{x} - \mathbf{y}\|_2^2$, $\{\mathbf{T}(\mathbf{f}_{1l})\}_{l=1}^{n_L}$ and $\{\mathbf{f}_{2k}\}_{k=1}^{n_k}$ are mapped samples and target samples, $\mathbf{T}(\cdot)$ is the map given by different methods, n_L is the length of each sample function and Π_{lk} is the probabilistic coupling. The experiments are indicted by $k_{source} \rightarrow k_{target}$, where k is the number of mixtures in the data. More mixtures implies a more complicated task. Here we use GPOT and LSOT as benchmarks; as demonstrated in Table 1, the push forward of FOT best matches the target sample functions quantitatively.

5.3. Optimal Transport for Robot Arm Multivariate Sequences

The trajectories of robot motion (joint states, positions) are intrinsically continuous functions of time. Due to the

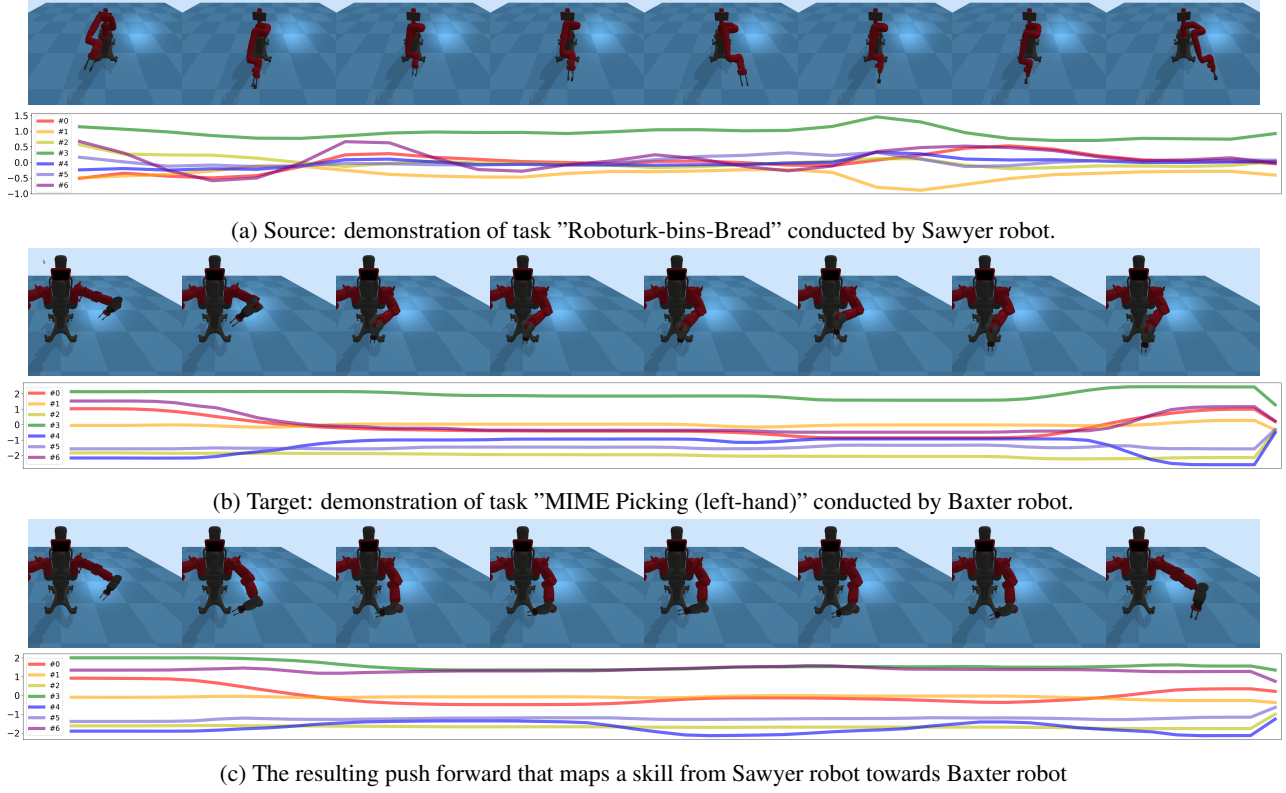


Figure 4: Visualization of robot tasks.



Figure 5: The arm of the Baxter robot and the Sawyer robot, used in the MIME dataset and Roboturk dataset respectively. They share a similar structure, 7 joints and one end effector.

uncertainty caused by sensors' noise, physical constraints and actuators, we can consider different trials of robot data on one task as multiple samples from one stochastic process.

MIME Dataset: The MIME Dataset (Sharma et al., 2018) contains 8000+ demonstrations across 20 tasks (e.g. pouring, book-closing, Stirring, etc.) collected on a Baxter robot. We select the tasks in which only one arm is used. For example, in the *pouring* task, the robot uses either its left arm or right arm. We therefore divide the data into *left-arm pouring* and *right-arm pouring*. We use the 7 dimensional joint angles of the robot arm as the dataset.

Roboturk Dataset: The Roboturk Dataset (Mandlekar et al., 2018) is collected by Sawyer robots on a number of different tasks (e.g. binning objects). As shown in Figure (5), the Sawyer robot only has one arm with 7 joints, leading to a 7 dimensional time sequences of joint angles.

Mapping robot demonstrations from one domain to another: Our method indeed learns a transport map that maps the trajectories from one dataset to the other. The source dataset is the demonstrations from task: *bins-full* of Roboturk dataset while the target is the demonstrations from task: *Pour(left-arm)* of MIME dataset. We visualize the demonstration by displaying the robot joint angles sequences in a physics-based robot simulation gym (Erickson et al., 2020). From Figure 4², we can see that the push-forward sequences matches with the target demonstration while it simultaneously preserves some feature of the source demonstration.

5.4. Domain Adaptation with Optimal Transport (for Robot-arm motion Prediction)

The recent progresses in robotics have witnessed a lot of novel approaches in reinforcement learning (Xu et al., 2020),

²More examples can be found here:

<https://sites.google.com/view/functional-optimal-transport>.

Method	R1 → M1	R1 → M2	R2 → M1	R2 → M2
LSTM	2.0217	1.6821	1.3963	1.1952
ANP	1.3261	1.0951	0.6642	0.6307
ANPRNN	1.9874	1.5681	1.7256	1.3659
MAML*	0.0307	0.0374	0.0327	0.0477
TL*	0.5743	0.7083	0.2491	0.4020
FOT _{MAML}	0.0165	0.0191	0.0202	0.0167
FOT _{TL}	0.0277	0.0446	0.0906	0.0406
FOT _{LSTM}	0.0271	0.0414	0.0277	0.0331
FOT _{ANP}	0.0963	0.1642	0.0951	0.1620
FOT _{ANPRNN}	0.0687	0.1331	0.0696	0.1554

Table 2: MSE error results of different predictive models. R1: Roboturk-bins-bread, R2: Roboturk-pegs-RoundNut, M1:MIME1-Pour-left, M2: MIME12-Picking-left.

motion prediction (Jetchev & Toussaint, 2009), and human robot interaction (Liu et al., 2018). However, generalizing knowledge from different tasks, from real-world to simulation, or from one domain to another are notoriously hard in robotic tasks. Therefore, a variety of approaches, such as domain adaptation (Bousmalis et al., 2018), domain randomization (Tobin et al., 2017), meta-learning (Finn et al., 2017), and transfer learning (Weiss et al., 2016) have been developed to tackle these problems.

Optimal Transport Domain Adaptation We apply our proposed method on an Optimal Transport based domain adaptation (OTDA) (Courty et al., 2016) for motion prediction. Our OTDA follows three steps: 1) learn an optimal transport map from the source to the target distribution, 2) map the observed source samples to match the target distribution and 3) train a motion predictor on the push-forward samples that lie in the target domain.

Datasets We also use the MIME dataset and the Roboturk Dataset. We pick 2 tasks *Pouring (left arm)* and *Picking (left arm)* from MIME dataset and 2 tasks (*bins-Bread*, *pegs-RoundNut*) from Roboturk dataset. We consider the demonstration data of each task as an individual domain.

Experiment Setup For the *Robot Arm Motion Prediction* task, a data of length l consists of a set of vectors $S_i \in \mathbb{R}^d$ with associated timestamps t_i . $S = (S_1, t_1), \dots, (S_l, t_l)$ where the time series trajectories are assumed to be governed by continuous functions of time $f_S(t) : t \in \mathbb{R} \mapsto S \in \mathbb{R}^d$. Since the task is to predict the future l_f points based on the past l_p points, therefore we can always arrange the data to have the format $X_t = \{(S_{t+1}, t+1), \dots, (S_{t+l_p}, t+l_p)\}$, $Y_t = \{(S_{t+l_p+1}, t+l_p+1), \dots, (S_{t+l_p+l_f}, t+l_p+l_f)\}$. Then our task is learning a predictive model that minimizes

the squared prediction error in the target domain

$$\arg \min_{\theta} \sum_{i=1}^M (F_{\theta}(X_i^t) - Y_i^t)^2 \quad (18)$$

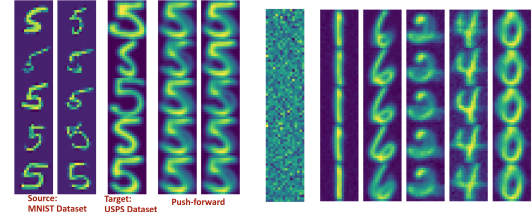
where Y_i^t is the true label from target domain and $\hat{Y}_i^t = F_{\theta}(X_i^t)$ is the predictive label estimated by a model trained on source domain (X^s, Y^s) and a subset of target domain (X^{tm}, Y^{tm}) .

Methods We consider 5 baselines to solve this task, including (1) a simple LSTM model only using the source data, (2) the Attentive Neural Process (ANP) (Kim et al., 2019), which is a deep Bayesian model that learns a predictive distribution over stochastic process, (3) the ANPRNN (Qin et al., 2019) a variant of ANP, (4) the Model-Agnostic Meta-Learning (MAML) model (Finn et al., 2017) applicable to a variety of tasks, and (5) a conventional transfer learning (TL) (Weiss et al., 2016) method, where we first train the model on source domain and then fine tune it on target domain.

The results are give in Table 2. Despite the difference of different approaches, we can see that FOT can significantly improve the performance of all downstream models.

5.5. High dimensional experiments

MNIST and USPS dataset We consider the MNIST dataset (LeCun et al., 1998) and the USPS dataset (Netzer et al., 2011) with the aim of learning an optimal transport map from one domain to another. Here the images are considered as surfaces such that $v = f(X)$, where $v \in \mathbb{R}$ is the pixel value, $X \in \mathbb{R}^2$ is the pixel index and $f : \mathbb{R}^2 \mapsto \mathbb{R}$ is a random function that generates one category of digit. We normalize the pixel value from $[0, 255]$ to $[0, 1]$. The results of the push-forward obtained by transport map are depicted in Figure 6a. We notice that the push-forward results of MNIST samples look like the target. Moreover, the push-forward inherit some features from the source.



(a) Mapping MNIST samples to USPS samples. (b) Generating digits from random noise

Figure 6: Qualitative result of FOT on high-dimensional digital number datasets.

Generative Optimal Transport Inspired by the corollary 1 of Seguy et al. (2017), the estimated Monge map can serve as a generator between an arbitrary continuous mea-

sure μ and a discrete measure ν representing the discrete distribution of the dataset.

6. Discussion

In order to learn an explicit transport map that pushes the sample functions from one stochastic process to another, we construct a map based on subspace approximation of Hilbert-Schmidt operator. The learned transport map shows its effectiveness on toy example datasets and real-world datasets. We believe that our approach paves the way for bridging optimal transport and functional data analysis techniques and practice.

References

- Arjovsky, M., Chintala, S., and Bottou, L. Wasserstein gan. *arXiv preprint arXiv:1701.07875*, 2017.
- Bhushan Damodaran, B., Kellenberger, B., Flamary, R., Tuia, D., and Courty, N. Deepjdot: Deep joint distribution optimal transport for unsupervised domain adaptation. In *Proceedings of the European Conference on Computer Vision (ECCV)*, pp. 447–463, 2018.
- Bousmalis, K., Irpan, A., Wohlhart, P., Bai, Y., Kelcey, M., Kalakrishnan, M., Downs, L., Ibarz, J., Pastor, P., Konolige, K., et al. Using simulation and domain adaptation to improve efficiency of deep robotic grasping. In *2018 IEEE international conference on robotics and automation (ICRA)*, pp. 4243–4250. IEEE, 2018.
- Chan, J., Miller, A. C., and Fox, E. B. Representing and denoising wearable ecg recordings. *arXiv preprint arXiv:2012.00110*, 2020.
- Courty, N., Flamary, R., Tuia, D., and Rakotomamonjy, A. Optimal transport for domain adaptation. *IEEE transactions on pattern analysis and machine intelligence*, 39(9): 1853–1865, 2016.
- Cuturi, M. Sinkhorn distances: Lightspeed computation of optimal transport. In *Advances in Neural Information Processing Systems*, 2013.
- Deisenroth, M. P., Fox, D., and Rasmussen, C. E. Gaussian processes for data-efficient learning in robotics and control. *IEEE transactions on pattern analysis and machine intelligence*, 37(2):408–423, 2013.
- Erickson, Z., Gangaram, V., Kapusta, A., Liu, C. K., and Kemp, C. C. Assistive gym: A physics simulation framework for assistive robotics. *IEEE International Conference on Robotics and Automation (ICRA)*, 2020.
- Finn, C., Abbeel, P., and Levine, S. Model-agnostic meta-learning for fast adaptation of deep networks. *arXiv preprint arXiv:1703.03400*, 2017.
- Ganin, Y. and Lempitsky, V. Unsupervised domain adaptation by backpropagation. In *International conference on machine learning*, pp. 1180–1189. PMLR, 2015.
- Genevay, A., Cuturi, M., Peyré, G., and Bach, F. Stochastic optimization for large-scale optimal transport. In *Advances in neural information processing systems*, pp. 3440–3448, 2016.
- Ho, N., Nguyen, X., Yurochkin, M., Bui, H. H., Huynh, V., and Phung, D. Multilevel clustering via wasserstein means. In *International Conference on Machine Learning*, pp. 1501–1509. PMLR, 2017.
- Horváth, L. and Kokoszka, P. *Inference for functional data with applications*, volume 200. Springer Science & Business Media, 2012.
- Hsing, T. and Eubank, R. *Theoretical foundations of functional data analysis, with an introduction to linear operators*, volume 997. John Wiley & Sons, 2015.
- Huang, C.-W., Chen, R. T., Tsirigotis, C., and Courville, A. Convex potential flows: Universal probability distributions with optimal transport and convex optimization. *arXiv preprint arXiv:2012.05942*, 2020.
- Huber, P. J. Robust estimation of a location parameter. *Annals of Statistics*, 53 (1):73–101, 1964.
- Jetchev, N. and Toussaint, M. Trajectory prediction: learning to map situations to robot trajectories. In *Proceedings of the 26th annual international conference on machine learning*, pp. 449–456, 2009.
- Kantorovitch, L. On the translocation of masses. *Management Science*, 5(1):1–4, 1958.
- Kim, H., Mnih, A., Schwarz, J., Garnelo, M., Eslami, A., Rosenbaum, D., Vinyals, O., and Teh, Y. W. Attentive neural processes. *arXiv preprint arXiv:1901.05761*, 2019.
- LeCun, Y., Bottou, L., Bengio, Y., and Haffner, P. Gradient-based learning applied to document recognition. *Proceedings of the IEEE*, 86(11):2278–2324, 1998.
- Liu, C., Tang, T., Lin, H.-C., Cheng, Y., and Tomizuka, M. Serocs: Safe and efficient robot collaborative systems for next generation intelligent industrial co-robots. *arXiv preprint arXiv:1809.08215*, 2018.
- Makkuva, A. V., Taghvaei, A., Oh, S., and Lee, J. D. Optimal transport mapping via input convex neural networks. *arXiv preprint arXiv:1908.10962*, 2019.
- Mallasto, A. and Feragen, A. Learning from uncertain curves: The 2-wasserstein metric for gaussian processes. In *Advances in Neural Information Processing Systems*, pp. 5660–5670, 2017.

- Mandlekar, A., Zhu, Y., Garg, A., Booher, J., Spero, M., Tung, A., Gao, J., Emmons, J., Gupta, A., Orbay, E., et al. Roboturk: A crowdsourcing platform for robotic skill learning through imitation. *arXiv preprint arXiv:1811.02790*, 2018.
- Masarotto, V., Panaretos, V. M., and Zemel, Y. Procrustes metrics on covariance operators and optimal transportation of gaussian processes. *Sankhya A*, 81(1):172–213, 2019.
- Meng, C., Ke, Y., Zhang, J., Zhang, M., Zhong, W., and Ma, P. Large-scale optimal transport map estimation using projection pursuit. *Advances in Neural Information Processing Systems*, 32:8118–8129, 2019.
- Mirshani, A., Reimherr, M., and Slavković, A. Formal privacy for functional data with gaussian perturbations. In *International Conference on Machine Learning*, pp. 4595–4604. PMLR, 2019.
- Mollenhauer, M., Schuster, I., Klus, S., and Schütte, C. Singular value decomposition of operators on reproducing kernel hilbert spaces. In *Proceedings of the Workshop on Dynamics, Optimization and Computation held in honor of the 60th birthday of Michael Dellnitz*, pp. 109–131. Springer, 2020.
- Netzer, Y., Wang, T., Coates, A., Bissacco, A., Wu, B., and Ng, A. Y. Reading digits in natural images with unsupervised feature learning. 2011.
- Perrot, M., Courty, N., Flamary, R., and Habrard, A. Mapping estimation for discrete optimal transport. *Advances in Neural Information Processing Systems*, 29:4197–4205, 2016.
- Qin, S., Zhu, J., Qin, J., Wang, W., and Zhao, D. Recurrent attentive neural process for sequential data. *arXiv preprint arXiv:1910.09323*, 2019.
- Rodrigues, F., Pereira, F., and Ribeiro, B. Gaussian process classification and active learning with multiple annotators. In *International conference on machine learning*, pp. 433–441. PMLR, 2014.
- Salimans, T., Zhang, H., Radford, A., and Metaxas, D. Improving gans using optimal transport. *arXiv preprint arXiv:1803.05573*, 2018.
- Seguy, V., Damodaran, B. B., Flamary, R., Courty, N., Rolet, A., and Blondel, M. Large-scale optimal transport and mapping estimation. *arXiv preprint arXiv:1711.02283*, 2017.
- Sharma, P., Mohan, L., Pinto, L., and Gupta, A. Multiple interactions made easy (mime): Large scale demonstrations data for imitation. *arXiv preprint arXiv:1810.07121*, 2018.
- Tobin, J., Fong, R., Ray, A., Schneider, J., Zaremba, W., and Abbeel, P. Domain randomization for transferring deep neural networks from simulation to the real world. In *2017 IEEE/RSJ international conference on intelligent robots and systems (IROS)*, pp. 23–30. IEEE, 2017.
- Villani, C. *Optimal transport: old and new*, volume 338. Springer Science & Business Media, 2008.
- Weiss, K., Khoshgoftaar, T. M., and Wang, D. A survey of transfer learning. *Journal of Big data*, 3(1):1–40, 2016.
- Xie, Y., Chen, M., Jiang, H., Zhao, T., and Zha, H. On scalable and efficient computation of large scale optimal transport. *arXiv preprint arXiv:1905.00158*, 2019.
- Xu, M., Ding, W., Zhu, J., LIU, Z., Chen, B., and Zhao, D. Task-agnostic online reinforcement learning with an infinite mixture of gaussian processes. *Advances in Neural Information Processing Systems*, 33, 2020.